Whole-Plant Physiological Identification and Quantification of Disease Progression

Shani Friedman[1], Ahan Dalal[1], Dor Batat[1], Saul Burdman[2], Yheonatan Sela[1], Matanel Hipsch[1], Shilo Rosenwaser[1], Evgeniya Marcos Hadad[2], Shay Covo[2] and Menachem Moshelion[1]

[1]The Robert H. Smith Institute of Plant Sciences and Genetics in Agriculture, The Hebrew University of Jerusalem, Rehovot 7610001, Israel

[2]The Institute of Environmental Sciences, The Robert H. Smith Faculty of Agriculture, Food and Environment, The Hebrew University of Jerusalem, Rehovot 7610001, Israel

Author for correspondence:

Menachem Moshelion

Tel.: +972 89489781

Email: menachem.moshelion@mail.huji.ac.il

	Word count	Figures and tables	Supporting information
Introduction	801		
Materials and Methods	2128		Fig. S1 – gray
Results	1690	Figs. 1, 4, 5 – color Figs. 2, 3 – gray Table 1 – color	Figs. S2, S3 – color Figs. S4, S5, S6 – gray Table S1 – color Model S1 – gray
Discussion	1837		
Acknowledgements	78		
Total	6456		

ORCIDs:

Menachem Moshelion - https://orcid.org/0000-0003-0156-2884

Shani Friedman - https://orcid.org/0009-0006-8663-0282

Saul Burdman - https://orcid.org/0000-0001-9544-7371

Summary

- Visual estimates of plant symptoms are traditionally used to quantify disease severity. Yet, the methodologies used to assess these phenotypes are often subjective and do not allow for tracking the disease's progression from very early stages. Here, we hypothesized that quantitative analysis of whole-plant physiological vital functions can be used to objectively determine plant health, providing a more sensitive way to detect disease.
- We studied the tomato wilt that is caused by *Fusarium oxysporum* f. sp. *lycopersici* (*Fol*). Physiological performance of infected and non-infected tomato plants was compared using a whole-plant lysimeter functional-phenotyping system. Water-balance traits of the plants were measured continuously and simultaneously in a quantitative manner.
- Infected plants exhibited early reductions in transpiration and biomass gain, which preceded visual disease symptoms. These changes in transpiration proved to be effective quantitative indicators for assessing both the plant's susceptibility to infection and the virulence of the fungus. Physiological changes linked to fungal outgrowth and toxin release contributed to reduced hydraulic conductance during initial infection stages.
- The functional-phenotyping method objectively captures early-stage disease progression, advancing plant disease research and management. This approach emphasizes the potential of quantitative whole-plant physiological analysis over traditional visual estimates for understanding and detecting plant diseases.

Key words:

Early detection, *Fusarium oxysporum* f. sp. *lycopersici*, leaf hydraulics, lysimeter, plant disease, whole-plant physiology

Introduction

Pathogens cause severe losses to agricultural production. Worldwide, an estimated 20–40% of crop yields are lost to pests and plant diseases (CABI, n.d.). Each year, plant diseases cost the global economy around $220 billion (Sarkozi, 2019). Therefore, monitoring plant health and detecting pathogens at an early stage are crucial for reducing pathogen establishment and spread, and for facilitating effective management practices in sustainable agriculture (Martinelli et al., 2015).

While in agriculture settings, disease severity is determined by yield or economic loss, in plant pathology research, the definition is more complex. Disease severity is the proportion of the plant unit exhibiting visible disease symptoms and is often expressed as a percentage value (Madden et al., 2007). The subjective visual estimations that are often used to quantify disease severity are prone to inaccuracy that can lead to incorrect conclusions (Bock et al., 2020; Stewart & McDonald, 2014). Accurate quantitative and objective assessment of plant disease severity is also critical for determining pesticide efficacy, correlating yield losses with disease damage, calculating damage thresholds and conducting reproducible experiments in any plant–pathogen interaction study. A quantitative method for studying disease progression would help us to understand the contribution of each determinant (plant, pathogen and environment) to the complex phenotype of a plant disease.

Healthy plants growing under optimal conditions adapt to environmental variations in ways that optimize their productivity. For instance, a healthy plant adeptly adjusts its stomatal opening to maximize CO_2 absorption when it is exposed to favorable ambient conditions, such as sufficient light, adequate soil moisture and optimal temperature. In contrast, a diseased plant will respond differently under identical conditions, potentially failing to exploit the environment to maximize its productivity potential. This disparity between a plant's inherent potential and its actual performance serves as the basis for our research hypothesis.

Plant-pathogenic fungi can decrease hydraulic conductance or transpiration in plants through various mechanisms. One mechanism is the disruption of water uptake and transport associated with the clogging of the xylem vessels by fungal mycelia (reviewed by Nemec et al., 1986). The secretion of polysaccharides and toxins by the fungus into the xylem, substances which are subsequently transported to the leaves, has been shown to reduce transpiration and

induce other physiological perturbations (Singh et al., 2017). Specific substances contributing to these effects include chitin (Attia et al., 2020) and fusaric acid (Dong et al., 2012).

We hypothesize that careful examination of subtle physiological changes (i.e., suboptimal functioning of the plant) that occur early in the infection process can provide insights into pathogen infection before the later emergence of visible symptoms. Furthermore, we hypothesize that suboptimal physiological parameters, such as transpiration, can signal failure resulting from the interaction with the pathogen in a more quantitative manner than visual assessment alone. However, this approach has not been widely used for early detection of disease (Bock et al., 2020; Fang & Ramasamy, 2015; Martinelli et al., 2015). Some studies have focused on the assessment of water-balance parameters to quantify and compare disease severity; however, those studies involved laborious, less-precise and time-consuming techniques (Dong et al., 2012; Wang et al., 2015). Gaunt (1995) previously suggested that adopting a simpler way to measure disease, based on deviations from normal plant function, could potentially resolve many of the challenges faced in linking disease with yield (Gaunt, 1995).

To test our hypothesis, we used high-throughput physiological phenotyping to detect early physiological responses to pathogen infection. Our whole-plant physiological monitoring approach provided detailed, simultaneous and continuous characterizations of whole-plant transpiration, biomass gain and other physiological traits at high resolution under dynamic soil and atmospheric conditions (Dalal et al., 2020; Halperin et al., 2017).

In this study, we focused primarily on the *Fusarium oxysporum* f. sp. *lycopersici* (*Fol*)–tomato pathosystem. *Fol* is a soil-borne fungus that spreads in the tomato plant through the vascular tissues, causing the plant to wilt. This phenomenon is assumed to be associated with both physical clogging of the xylem vessels and toxins secreted by the fungus into the xylem (Kashyap et al., 2021). Physical and chemical barriers contribute to vascular blockage, disrupting plant water-balance and promoting wilting (Kashyap et al., 2021). Given *Fol*'s significant impact on water-related physiological traits, we hypothesized that these traits might serve as early markers of infection in the leaf and the whole plant. In addition to the *Fol*–tomato pathosystem, we also examined late blight disease (*Phytophthora infestans* Mont. DeBary) of potato (*Solanum tuberosum*). We aimed to test our method's capability for detecting disease in other plant–microbe interactions. Simultaneously, we also investigated plant infection levels using traditional techniques. Traditional methods such as PCR, visual-symptom analysis and post-harvest tests

were utilized to confirm the presence of pathogens. This work might contribute to a broader understanding of plant–pathogen–environment interaction and help to improve the methods available for studying vascular wilt diseases.

Materials and methods

Plant material and growth conditions

Plant material

Tomato cultivars with different susceptibility to *Fol* race 2 were tested, including the industrial cultivar *Lycopersicon esculentum* cv. M82 (Eshed & Zamir, 1995) that is tolerant of the pathogen (Sela-Buurlage et al., 2001) and the cultivars Rehovot-13 (Hazera Genetics, Brurim Farm, Israel) and Marmande Verte, which are susceptible to this pathogen. In addition, we used the nearly isogenic tomato cultivars Moneymaker and Motelle, which are susceptible and resistance to *Fol* race 2, respectively (Sarfatti et al., 1989). 'Marmande Verte' and 'Motelle' seeds were kindly provided by Y. Rekah (Hebrew University , Israel) and were originally obtained from H. Laterrot (INRA, France). In addition, wild-type potato cv. Desiree expressing chloroplast-targeted roGFP2 was also used in the study (Hipsch et al., 2021).

Greenhouse conditions

This work was performed in a greenhouse located at the Robert H. Smith Faculty of Agriculture, Food and Environment, Hebrew University (Rehovot, Israel), which is an extension of the I-CORE Center for Functional Phenotyping greenhouse (http://departments.agri.huji.ac.il/plantscience/icore.phpon) for plant disease research. The greenhouse allows natural day length and light conditions and has a desert cooler along its northern wall to prevent overheating. Continuous environmental data, such as PAR light, temperature, relative humidity and vapor pressure deficit, were monitored continuously and recorded every 3 min (Fig. S1).

Plant physiological phenotyping

Whole-plant, continuous physiological measurements were taken using load cells (lysimeters) which are specially designed for plant physiology screening (PlantArray 3.0 system; Plant-DiTech, Yavne, Israel). (For more information, please see Dalal et al., 2020; Halperin et al., 2017). In the greenhouse, there were 36–60 highly sensitive PlantArray units, which collected data and controlled the irrigation for each pot separately. The data were analyzed using SPAC-

analytics (https://spac.plant-ditech.com), a web-based software program that allows analysis of the real-time data collected from the PlantArray system (Halperin et al., 2017).

Tomato seeds were germinated in cavity trays in the greenhouse. Three- to 4-week-old tomato plants were inoculated (as described below) and then transplanted into 4-l pots filled with quartz sand 20/30 (min/max nm; Negev Industrial Minerals Ltd., Yeruham, Israel) or commercial growth medium (Matza Gan; Shacham, Givat-Ada, Israel). Pot, sand and plants were weighed ahead of the experiment and the tare weight was taken. On the day of transplanting, the soil was kept saturated to ensure the plants' establishment and, from then on, irrigation was applied only at night. The pots were covered with a custom cover that only allowed the stem through it, to minimize evaporation.

Transpiration, plant weight and E

Transpiration, plant weight and transpiration rate and E (calculated in terms of water transpired per unit of plant net weight per min) values are essential water-relations kinetics and quantitative physiological traits (Dalal et al., 2020; Halperin et al., 2017). Plant weights were calculated daily after the pots were fully watered and drained, when the plants were at full turgor. Transpiration, referred to as 'daily transpiration' or 'transpiration rate', was calculated based on the weight loss during the day.

Determination of leaf hydraulic conductance (K_{leaf})

Tomato plant leaflets that were approximately 1.5 to 2 months old (among the first three leaflets from top younger leaves of similar size) with no noticeable injuries or anomalies were excised before dawn and were immediately dipped in a 2-ml tube, with their petioles dipped in artificial xylem solution (AXS; Attia et al., 2020) with or without 10 µM abscisic acid (ABA) or 0.2 mg ml^{-1} of chitin [a 10 mg ml^{-1} stock solution was prepared according to Attia et al., 2020)], or with 0.5% of the sterile concentrated fungal culture filtrate or control filtrate (described below), and exposed to a light intensity of 150 µmol m^{-2} s^{-2} at 26–28°C. Transpiration from each perfused leaf and its water potential were measured between 2–4 h of treatment using an Li-600 porometer (LI-COR, Bnei Brak, Israel) and pressure chamber (Arimad-3000; MRC Ltd., Holon, Israel), respectively, as described previously (Grunwald et al., 2021). Leaf hydraulic conductance (K_{leaf}) was calculated as the negative of the ratio of transpiration to water potential (Grunwald et al., 2021).

Pathogen material and growth conditions

Fungal strains and growth conditions

Two isolates of *Fol* race 2 were used: *Fol* 4287 obtained from the American Type Culture Collection (ATCC) and fr2T obtained from Hazera Genetics. In preliminary experiments, *Fol* 4287 was found to be a moderately virulent strain (mvF) and fr2T was found to be a highly virulent strain (vF). The fungi were grown on plates containing potato dextrose agar (PDA) with 2% Bacto Agar (Difco, MD, USA). For formation of microconidia, the strains were grown in a liquid minimal medium (LMM) that contained 100 mM KNO_3, 3% sucrose and 0.17% yeast nitrogen base without amino acids (R. Cohen et al., 2019). *Fol* was cultured in 500-ml Erlenmeyer flasks containing 50 ml LMM. The Erlenmeyer flasks were incubated for 6 d at 28°C with rotary shaking at 185 rpm. The resulting fungal cultures were filtered through a 40-µm strainer (Corning, Cell Strainer; Sigma-Aldrich, Rehovot, Israel) to remove the mycelia and then centrifuged at 3220 g for 10 min to pellet the conidia. The conidia were resuspended in sterile water and quantified using a Neubauer hemocytometer counting chamber (Mariefeld, Lauda-Königshofen, Germany) under a Nikon H550S microscope (Nikon, Tokyo, Japan). *Fol* was stored for long periods at −80°C, in aliquots containing 30% glycerol and a million cells ml^{-1}.

***FoI* inoculation**

The plant roots were washed and trimmed to obtain more uniform and homogeneous infection. The roots were then submerged in a suspension containing *Fol* (10^7–10^6 conidial spores ml^{-1} distilled water) for 5–10 min. The plants were then transplanted into well-irrigated pots. Control plants were treated similarly, except that sterile water was used instead of the conidial suspension.

***Phytophthora infestans* inoculation**

Isolate 164 of *Phytophthora infestans* (genotype 23_A1, resistant to mefenoxam) was used in this experiment. This pathogenic oomycete was collected in March 2016 from a potato field in Nirim, in the western Negev, Israel (Y. Cohen, 2020). *P. infestans* was propagated in a growth chamber at 18°C by repeated inoculations of freshly detached potato leaves. For inoculation, freshly produced sporangia were collected at 5–7 days after inoculation (dai) from infected leaves by washing with distilled water (DW) into a beaker kept on ice (4°C).

Potato (*Solanum tuberosum* cv. Desiree) plants were vegetatively propagated from cuttings or tubers and placed in moist soil in 26.82 × 53.49 cm pots within a controlled

environment greenhouse. Four-week-old plants were cultivated from cuttings in 4-l pots filled with sandy soil and, for the experiment, 3- to 4-week-old plants were transferred from the controlled-environment greenhouse to the I-CORE facility.

We inoculated the potato plants by spraying their foliage with a fresh suspension of *P. infestans* (genotype 23_A1) sporangia (1×10^5 sporangia ml^{-1}). The plants were then wrapped in black plastic bags and incubated in the dark for 18 h until the next morning, at which point the bags were removed (Hipsch et al., 2023). Plants sprayed with DW served as the control.

Preparation of fungal-culture filtrate toxin

We prepared *Fol* filtrate toxin, to evaluate its impact on leaf hydraulics. The *Fol* strains were cultured in Czapek Dox media, as described in previous studies (Portal et al., 2018; Scala et al., 1985; Sutherlandt & Pegg, 1992). Briefly, the strains were inoculated into 50 ml of Czapek Dox media, which was then incubated on an orbital shaker set at 130 rpm in darkness for 14 days at 25°C. The culture filtrate (CF) was then filtered through Whatman filter paper and concentrated up to approximately 10% of initial volume by rotary evaporation at 25°C. The concentrated CF preparations were filtered through 0.45-µm sterile syringe filters, to remove any spores or mycelial fragments that might cause physical blockage during the petiole-fed treatments for the hydraulic experiment. For the control treatment, the same procedure was followed without any inoculation. In the hydraulic experiment, 0.5% of the sterile concentrated CF or control filtrate was used as the working concentration.

Assessment of disease

Mature-plant assays

Disease severity was monitored continuously (daily) and was scored with the following symptom severity scale: 0, asymptomatic plants; 1, weakly infected plants (<25% of leaves chlorotic or wilted); 2, moderately infected plants (25–50% of leaves were chlorotic or wilted); 3, highly infected plants (>50% of the leaves wilted, but plants were alive); and 4, dead plants. The area under the disease progress curve (AUDPC) per pot was calculated. At the end of the experiment, 3–4 weeks after inoculation, we measured both the fresh weight and the height of the plant shoots and, in some cases, the roots as well.

Seedling assays

Tomato seeds were sown in vermiculite V2U (Agrekal, Moshav Habonim, Israel) and seedlings were grown for 10–13 days in a temperature-controlled glasshouse with a maximum daytime

temperature of 25°C and minimum nighttime temperature of 18°C prior to fungal inoculation. *Fol* cultures were grown and filtered as described above. Seedlings were removed and their roots were washed with water, trimmed, and then dipped in a conidial suspension (16×10^6 conidia ml^{-1}) for 5 min before being replanted in a mixture of vermiculite with autoclaved soil (4 units vermiculite:1 unit soil). Roots of control plants were dipped in water for the purposes of mock inoculation, to ensure that disease phenotypes were a consequence of *Fol* infection rather than the inoculation process per se. Plants were grown in trays; each tray contained both susceptible plants (cv. Moneymaker) and resistant (cv. Motelle) controls to ensure infection. To ensure successful infection and development of disease symptoms, the seedlings were densely planted and covered with foil for 2 days, with no fertilizer applied. Plants were kept in a controlled-environment growth room that was kept at 27°C, with a 16/8 h day/night cycle.

After 18 or 21 days, wilt symptoms and vascular browning were recorded and used to calculate disease scores according to criteria similar to those described by Rep et al. (2007): 0, healthy plant; 1, one or two brown vascular bundles in hypocotyl; 2, at least two brown vascular bundles and growth distortion; 3, all vascular bundles are brown; plant either dead or very small and wilted (Supplementary Fig. 2).

Pathogen-progress assays

For each plant, stem pieces were collected 0, 5 and 15 cm from the soil surface. These stem pieces were then surface-sterilized by submerging them in 70% ethanol and exposing them to an open flame. A slice of each sterilized stem piece was put on a plate filled with PDA supplemented with 250 mg l^{-1} streptomycin or 100 µg ml^{-1} ampicillin to reduce bacterial contamination (van der Does et al., 2019). After 4 days of incubation in the dark at 28°C, fungal outgrowth was assessed using a double-blind method, in which the people examining the sample did not know the treatment status of each sample and therefore were not biased.

Molecular pathogen assays

Fungal strains were grown for 5 days in PDA at 28°C under static conditions. Mycelia were harvested and ground with pestle and mortar with liquid nitrogen. Samples were stored at -20°C overnight. Genomic DNA extraction was carried out using either the Hi PurATM Fungal DNA Mini Kit (HiMedia, India), following the manufacturer's instructions, or the CTAB method (Muraguchi et al., 2003; Zolan & Pukkila, 1986).

The DNA samples were stored at −20°C for further use. Samples of genomic DNA (3 µl) were added to PCR tubes containing 22 µl PCR Mastermix with appropriate primers (as described below), PCR-grade H_2O and RedTaq Ready Mix according to the manufacturer′s instructions (Sigma-Aldrich, Rehovot, Israel). The amplified products were subjected to electrophoresis on 1.2% agarose gel containing agarose in 0.5 X TBE buffer and were stained with ethidium bromide. Gel images were captured using a C200 gel imaging workstation (Azure Biosystems; Dublin, CA, USA).

The amplification protocol used for the PCR reactions included an initial denaturation at 94°C for 1 min, followed by 25 cycles of denaturation at 94°C for 1 min, annealing at 58°C for 30 s, extension at 72°C for 1 min and a final extension at 72°C for 7 min.

The target genes amplified were the *six5* gene for *Fol* (product size: 667 bp) and the ITS region (product size: 340 bp). The *six5* gene primers were as follows: *six5*-f1 (ACACGCTCTACTACTCTTCA) and *six5*-r1 (GAAAACCTCAACGCGGCAAA) (Taylor et al., 2016). The primers for the ITS region were: FOF (ACATACCACTTGTTGCCTCG) and FOR (CGCCAATCAATTTGAGGAACG) (Prashant et al., 2003).

Statistical analyses

We used the JMP® ver. 16 statistical packages (SAS Institute, Cary, NC, USA) for our statistical analyses. Student's *t*-test was used to compare the means of two groups and ANOVA was used to compare means among three or more groups. Levene's test was used to examine the homogeneity of variance among the treatments. Differences between the treatments were examined using Tukey's HSD test. Each analysis involved a set significance level of $P < 0.05$.

Results

Early detection and quantification of plant pathogen interactions: Insights from the PlantArray system

This research focused on the use of the PlantArray system to detect and quantify early signs of disease in plant–pathogen interactions. This study primarily involved two strains of *Fusarium oxysporum* f. sp. *lycopersici* (*Fol*): a moderately virulent strain (mvF) and a highly virulent strain (vF) isolated from diseased tomato. The selection of strains was validated through a standard seedling infection assay (Fig. S2). The seedlings infected with vF exhibited significantly more severe symptoms than those infected with mvF (Fig. S3). It is important to note that these

assessments were terminal, as they required the physical cutting of plants for internal examination, and the severity of symptoms was subjectively scored in arbitrary units.

Further investigation of the virulence of these strains was conducted using the PlantArray system (Fig. 1a). This involved assessing the effects of mvF and vF inoculation of the *Fol*-susceptible cv. Rehovot-13 (R13) plants (Fig. 1b). Tomato plants that were 26 days old were inoculated with either vF or mvF and grown under well-irrigated greenhouse conditions. The PlantArray system was utilized for continuous monitoring of critical physiological parameters, including transpiration and plant biomass gain. Both *Fol* strains significantly reduced daily transpiration rates in the plants (Fig. 1c), leading to wilt symptoms in the R13 plants (Fig. 1d,e). The impact of vF was more pronounced than that of mvF, with a noticeable reduction in transpiration seen as early as 16 days after inoculation (dai), which was 6 days before similar observations in mvF-inoculated plants. This was coupled with a higher overall disease severity in the case of vF-inoculated plants (Fig. 1).

We conducted several independent repetitions with these strains, inoculating different tomato cultivars (Table 1). However, in 11 out of 19 experiments (Table S1), no visible symptoms or alterations in transpiration were observed, despite successful infection that was confirmed by fungal outgrowth tests. In 7 out of 8 cases where symptoms were observed (reduction in daily transpiration, reduction in plant weight, or visual symptoms), the infection was first detected by a reduction in daily transpiration, followed by other parameters (Table 1).

The first evidence of disease in the R13-inoculated plants was consistently a reduction in daily transpiration (6–22 dai), followed by a decrease in plant weight (19–32 dai) and, eventually, visible symptoms (21–60 dai; Table 1). No visible symptoms were evident when physiological symptoms first became significant (Fig. 1a). Inoculation of the more tolerant plants, M82, with strain mvF did not cause any visible or physiological symptoms. Nevertheless, the highly virulent vF did affect the M82 plants physiologically, as in all other cases, with infection first detected as a change in transpiration and later as an effect on plant net weight (Table 1), yet no visible morphological symptoms were detected over the course of the experiment.

At the end of every experiment, we documented the physical condition of the plants (Fig. 2a,b). To validate *Fol* infection, we also conducted a series of post-harvest analyses. These included cutting the plant at the stem base to assess the browning of the vascular system (Fig.

2c), a typical symptom induced by *Fol* in tomato. Next, we performed fungal outgrowth tests, to assess whether the fungus was present in the stem. In the experiments presented in Table 1, the outcome matched the treatments (Fig. 2d). Finally, PCR tests were conducted on some of the fungal outgrowth colonies to verify *Fol*'s identity (Fig. 2e). The aforementioned assays provided evidence that the inoculum was successful and that the fungi colonized the inoculated plants independently of changes in physiological parameters.

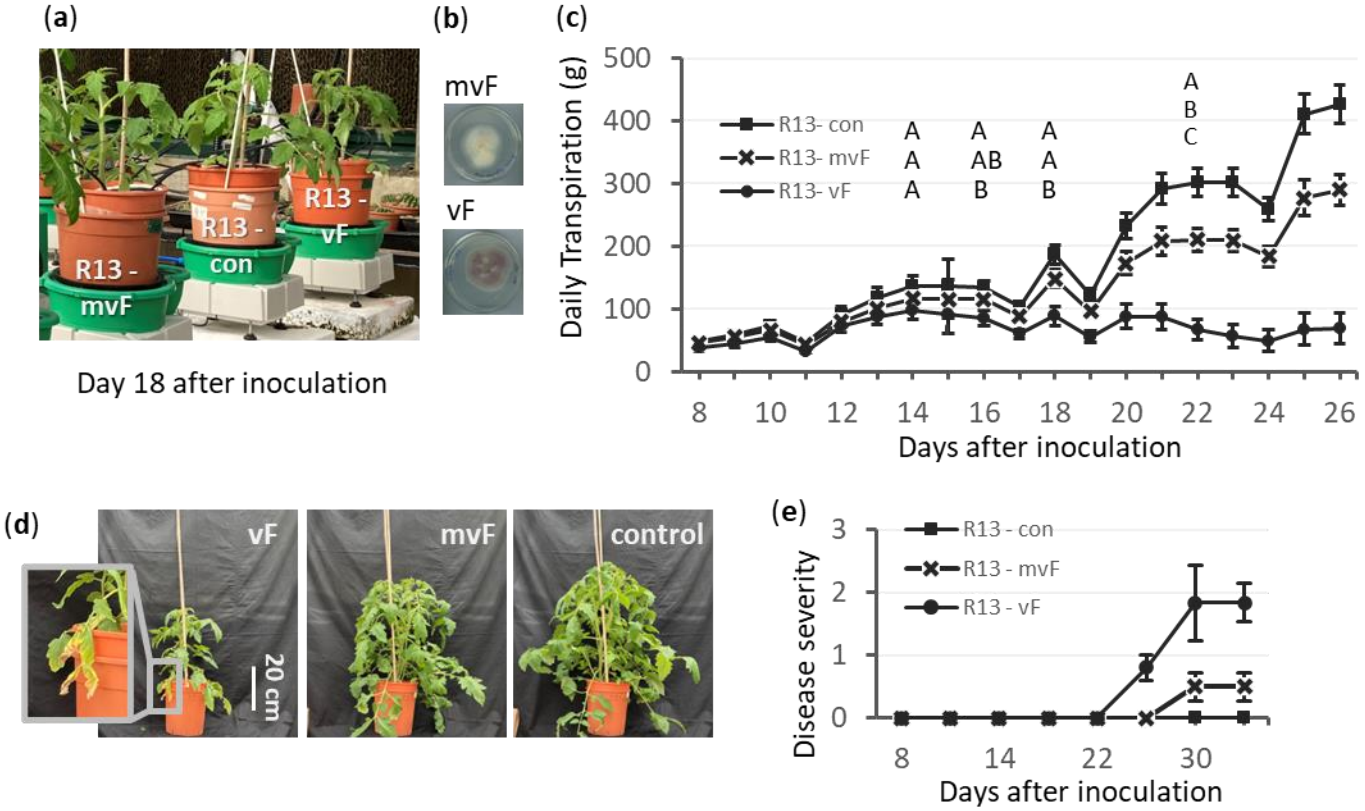

Fig. 1 Variations in transpiration corresponded to virulence levels prior to visible signs of disease. Rehovot-13 (R13) susceptible plants infected with either mvF (common strain) or with vF (virulent strain) were compared with control (mock-infected plants). (a) Plants at Day 18 in the PlantArray system. (b) At the end of the experiment, stem pieces were incubated on PDA plates. The outgrowth of fungi was transferred to new plates; mvF fungi were pink while vF fungi were violet. All infected plants showed stem browning and fungal outgrowth, while none of the controls did. (c) Daily transpiration of the whole plants (mean ± SE), different letters indicate a significant difference between treatments; $p \leq 0.05$. (d) Plants at the end of the experiment (Day 39 after inoculation). (e) Disease progress curve, error bars indicate SE. Average of wilt symptoms evaluated using the disease-severity index mentioned in the Materials and Methods. $n = 6$.

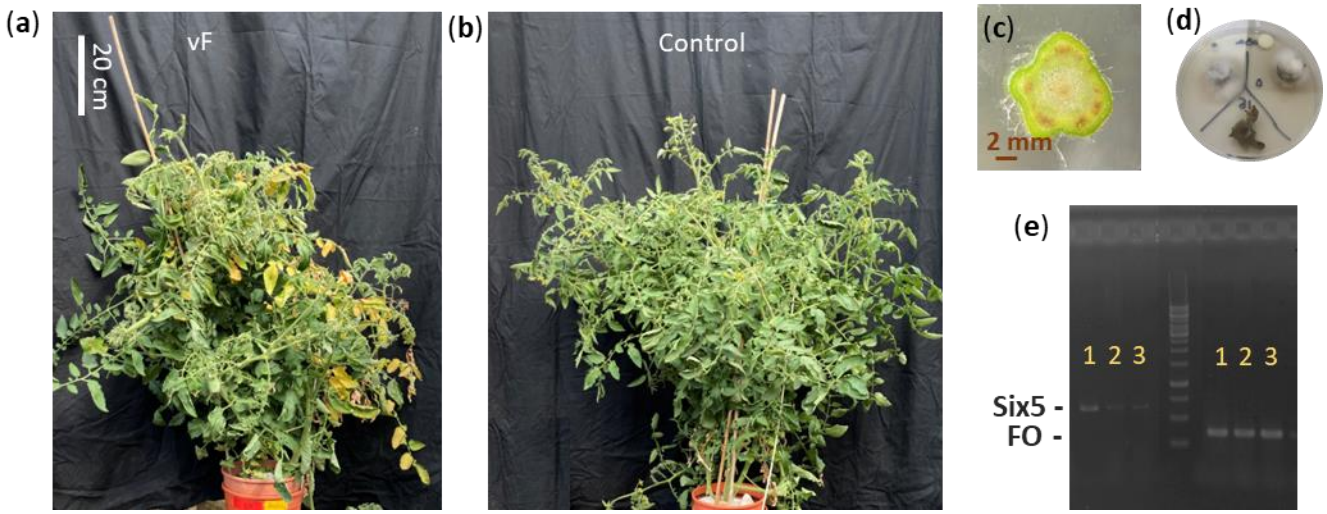

Fig. 2 Tests to confirm infection. (a) Visual symptoms of a *Fol*-inoculated Rehovot-13 plant, including wilting and typical chlorosis at 68 dai. (b) Control Rehovot-13 plant. (c) Browning of the vascular system in an inoculated plant, indicating fungal colonization. (d) Fungal outgrowth from stem cutting of an inoculated plant observed on a PDA plate. (e) Representative fungal outgrowth was subjected to PCR analysis to confirm the presence of *Fol* using the Six5 gene (667 bp) and FO ITS region (340 bp).

Table 1 Summary of Fol–tomato experiments: Transpiration, weight and morphology symptoms

Experiment		**Treatment**		**Symptoms**			
Exp.	Months	*Fusarium*	Tomato	Transpiration[1]	Weight[1]	Morphology[2]	End exp.
2	May-Jun	mvF	M82	-	-	-	25 days
6	Dec	mvF	M82	-	-	-	39 days
5A	Oct-Nov	vF	M82	18 days	31 days	-	39 days
6	Dec	vF	M82	24 days	35 days	-	39 days
11	Apr	vF	MM	13 days	17 days	-	19 days
5B	Oct-Nov	mvF	R13	6 days	19 days	21 days	75 days
4	Aug	mvF	R13	11 days	25 days	60 days	34 days
6	Dec	mvF	R13	22 days	32 days	32 days	39 days
6	Dec	vF	R13	16 days	25 days	28 days	39 days
9	Jan	vF	MV	22 days	7 days	35 days	42 days

The plants tested included M82 (tolerant), R13 (susceptible), Mv (susceptible) and MM (susceptible). Plants were inoculated with either the moderately virulent strain (mvF) or the highly virulent strain (vF).

[1] "Transpiration" and "weight" columns indicate the point in time (dai) at which a *t*-test revealed a significant difference from the control; $p < 0.05$.

[2] "Morphology" column indicates the point in time (dai) at which 50% of plants exhibited chlorosis or wilting.

To assess the tolerance of tomato cultivars to *Fol* (vF), we compared inoculated and non-inoculated R13 and M82 plants, to quantify their overall physiological responses to *Fol*. The analysis of these quantitative parameters allowed us to calculate relative losses (as depicted in Fig. 3a,b). We found that M82 plants exhibited a relatively high level of physiological tolerance, experiencing only a 15% decrease in weight, as compared to non-inoculated controls. In contrast, the R13 plants displayed a more susceptible physiological response, with markedly pronounced losses, resulting in a 67% decrease in weight compared to controls. Additionally, we observed disparities in basic vigor traits between the two varieties, with the R13 plants exhibiting faster growth and accumulating more biomass than the M82 plants (Fig. 3b).

Subsequent tests were carried out on various tomato cultivars, to evaluate the efficacy of the system across varieties differing in their levels of resistance to *Fol*. We specifically examined the performance of cv. Motelle (MT), a cultivar known to be highly resistant to *Fol*, cv. Moneymaker (MM), which is nearly isogenic to MT yet susceptible to *Fol*, and the *Fol*-susceptible cultivar Marmande Verte (MV). Consistent with our earlier findings, we observed a reduction in transpiration in infected MV plants (Fig. 3c). Moreover, the decrease in transpiration, expressed as a percentage of the daily maximum transpiration (Fig. 3d), provided a clear and quantitative measure of the functional losses among the different groups. Specifically, the MV plants infected with vF transpired only 10% of the daily maximum.

Fol-inoculated MM plants transpired significantly less and also gained less biomass than non-inoculated MM plants (about 20% less transpiration; Fig. S4). Non-inoculated MM plants showed a trend of increased productivity relative to MT plants, but that difference was not significant (Fig. S4). As expected, the resistant MT plant did not exhibit a significant change in weight or transpiration despite *Fol* inoculation.

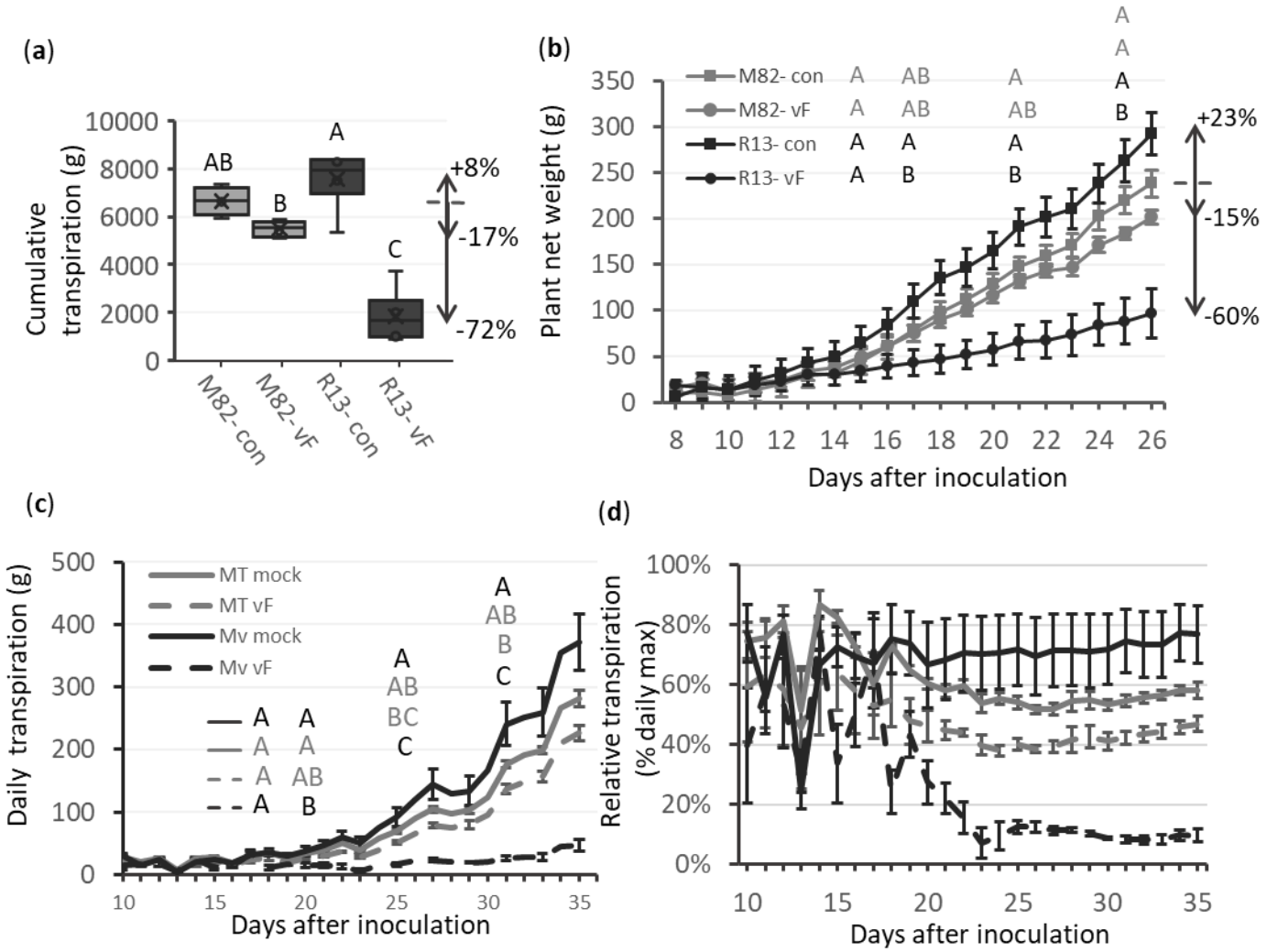

Fig. 3 Differential impact of inoculation on water balance in resistant and susceptible plants: Profiling plants' responses to Fol inoculation. Plants were inoculated with virulent *Fol* strains (vF) or mock-inoculated (control). (a) This box-and-whisker plot represents the cumulative transpiration, which indicates the total water lost by the plants over the course of the experiment. Tolerant M82 plants are represented in gray, while susceptible Rehovot-13 (R13) plants are depicted in black. (b) Plant weight (mean ± SE) over the experimental period. M82 is shown in gray; R13 is shown in black; circles indicate inoculated plants, while squares indicate non-

inoculated, control plants. The differences between each set of plants and the M82-control (dashed line) at the end of the experiment are presented as arrows and percentages. (c) Daily transpiration (mean ± SE) over the experimental period. Resistant cv. Motelle (MT) plants are shown in gray and susceptible cv. Marmande Verte (Mv) plants are shown in black. Dashed lines indicate inoculated groups. Using the same data, we calculated the (d) daily transpiration relative to the daily maximum values (mean ± SE). Different letters indicate statistically significant differences (p = 0.05; Tukey-Kramer test).

Reduction in transpiration due to *Fol* infection may be due to fungal hyphae clogging the xylem vessels, thereby reducing their hydraulic conductance. Yet, the relatively rapid reduction in transpiration symptoms that we observed (Table 1) suggests that fungal toxins and/or chitin released into the vascular system could be involved, potentially triggering a signal transduction pathway that reduces hydraulic conductance at an early stage of infection. To assess the effect of isolated culture-filtrate toxins on leaf hydraulic conductance (K_{leaf}), we compared the impact of fungal culture filtrate, perfused into the leaf vascular system, with control treatments of chitin and ABA. Both the susceptible MM and the resistant MT plants exhibited similar reductions in K_{leaf} when exposed to control stress-treatments of chitin and ABA (Fig. 4a; 48% and 89%, respectively). These results are consistent with findings reported in previous studies (Attia et al., 2020). However, the susceptible MM cultivar showed a significantly greater decrease in K_{leaf} in response to the highly toxic-treated group (vF ; 65%), as compared with the moderately toxic group (mvF; 42%), and a significant reduction in K_{leaf} as compared to the MT cultivar in response to both of these treatments (Fig. 4b). Specifically, MT plants showed a 25% reduction in K_{leaf} when infected with mvF and a 35% reduction when infected with vF. This decrease in K_{leaf} suggests a strong response to the presence of fungal toxins, which may implicate these toxins in the mechanism that reduces K_{leaf}.

Additionally, we observed substantial reductions in the leaf transpiration rate (E) and leaf water potential (Ψ_{leaf}) following treatment with stress-controls chitin and ABA in both MT and MM plants (Fig. S5). Furthermore, similar to our whole-plant results, the MM cultivar exhibited a significant reduction in leaf E under the mvF treatment, which became even more pronounced under the vF treatment (24% and 43%, respectively). In contrast, the MT cultivar did not show any reduction in leaf E under the mvF treatment and its reduction of E under the vF treatment was less pronounced than that of the MM plants (18%, Fig. S6).

We also tested the potential of the PlantArray system for early detection of disease in potato caused by *P infestans*. The initial symptoms of this disease are irregular spots that are light to dark green in color, moist in appearance and necrotizing. These lesions appeared 4 to 5 dai (Fig. 5e, Day 7). The daily transpiration and plant net weight were significantly different at 5 dai (Fig. 5a,b). However, it took only 3 days from infection for significant differences in transpiration and E (transpiration normalized to weight) at midday to develop between the control and the infected plants (Fig. 5c,d). These findings suggest that transpiration changes can also be indicative of non-vascular diseases, further underlining their utility as a broad-spectrum indicator of plant health issues. Moreover, these findings strengthen the claim that transpiration is a highly sensitive physiological trait that could be used to detect early disease symptoms and assess plant health.

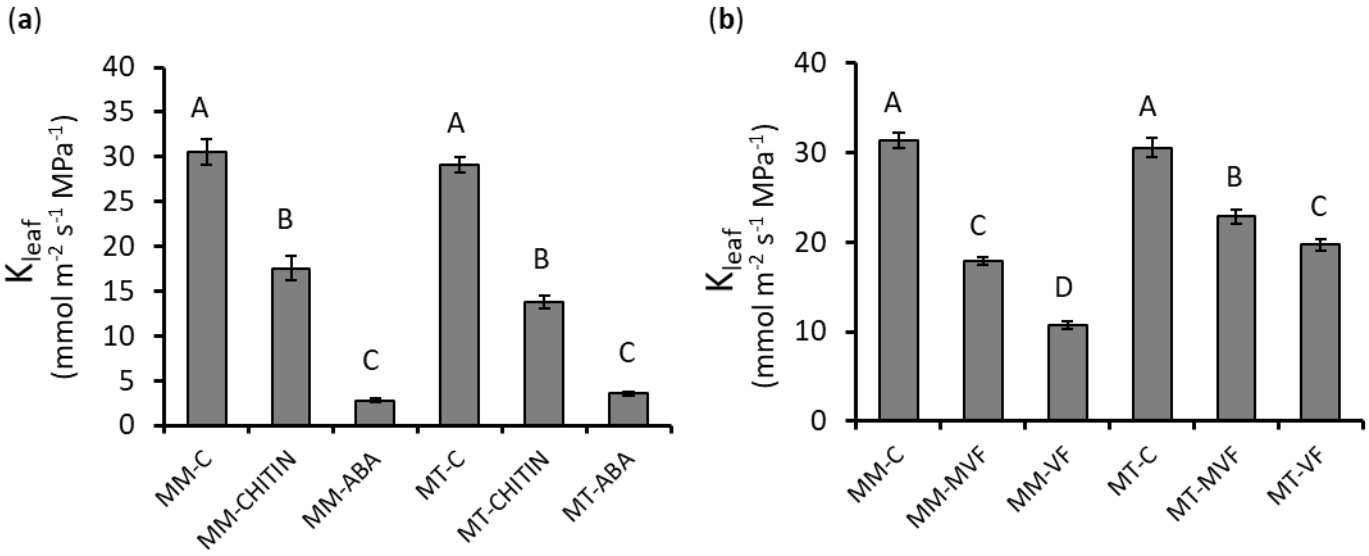

Fig. 4 Effects of chitin, ABA and fungal toxins on leaf hydraulic conductance (K_{leaf}). Detached leaves from cv. Moneymaker (MM) and cv. Motelle (MT) tomato plants were treated for 2–4 h with: (a) chitin (0.2 mg/ml) or ABA (10 μM) or (b) toxins released to the medium during fungal growth from both moderately virulent and virulent *Fol* strains. Control groups were fed with AXS alone. MVF and VF: Treated with toxins from the moderately virulent and virulent *Fol* strains, respectively. Different letters indicate significant differences between treatments according to the

426 Tukey-Kramer HSD test ($P < 0.05$). Data points are means (± SE) from 3 to 5 distinct experiments,
427 including 12–30 biological repetitions.

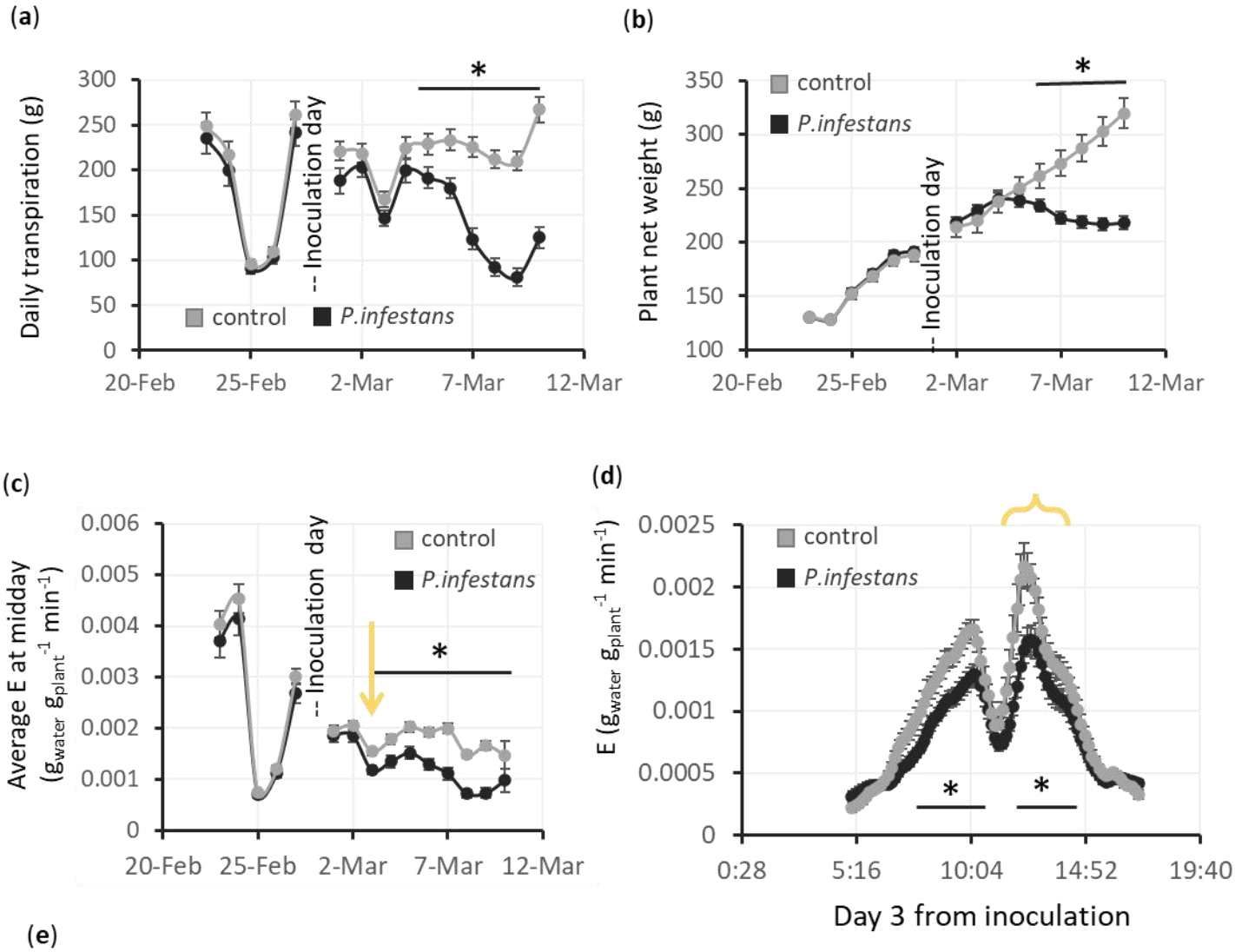

428

Fig. 5 Quantitative early detection of *Phytophthora infestans* in potato. Potato plants inoculated with *P. infestans* were compared with control (mock-infected) plants. Inoculation day was 28-Feb; Day 1 after inoculation was 1-Mar. (a) Daily transpiration of the whole plants, means ± SE. (b) Plant net weight over the entire experimental period, means ± SE. (c) Daily average E between 11:00–14:00. At this time of day, E is usually at its highest. (d) E values throughout the third day from inoculation, means ± SE. The orange arrow and bracket are pointing at the same data represented as point or continues data, respectively. Each treatment had 18 plants, asterisks indicate significant differences between the inoculated and control groups (*t*-test; $p < 0.05$). (e) Pictures of inoculated plants at different points in time after inoculation.

Prediction of disease symptoms in infected plants: Biotic and abiotic interplay

To identify the factors influencing the occurrence of disease symptoms in infected plants, we examined various internal and external factors (Table S1). Our automated system efficiently collected this information, enabling the generation of a detailed dataset encompassing environmental conditions, infection parameters and plant properties. We entered these data into a model to predict the occurrence of disease events with symptoms. Specifically, we focused on the interaction between cultivar and fungal strain, as well as plant properties on the date of inoculation, such as weight and age. Additionally, we examined the impact of the environmental parameters at 3 dai that were automatically collected from the PlantArray system, including temperature, relative humidity (RH) and daily light integral (DLI). We only included experiments in our analysis where the infected plants showed fungal outgrowth at the post experiment analysis, indicating successful infection (Table S1, “Fungi test”). By employing logistic regression analysis and a backward elimination approach, we identified the best model for predicting whether disease symptoms would appear (Model S1). The model demonstrated a high degree of accuracy ($R^2 = 1$, Pv < 0.0001). The significant variables in this model include the interaction between the plant cultivar and fungal strain (Pv = 0.011), plant initial weight (Pv < 0.001), RH (Pv < 0.001) and DLI (Pv < 0.001). Furthermore, our findings suggest that smaller plant weights (coefficient of -52.64, not significant), higher RH (coef. 58.24, n.s.) and higher DLI (coef. 34.1, n.s.) during the initial 3 days are associated with an increased likelihood of the development of disease symptoms in infected plants. However, it is important to note that the observed coefficients had high chi-square values (ChiSq = 0), but lacked statistical significance (Pv = 0.99), likely due to the limited number of repetitions within each plant–pathogen group.

Discussion

Visual estimation is the main method used to detect and assess plant diseases. However, the fact that visual estimation often relies on subjective assessment and the late appearance of visible symptoms limit the efficiency of that approach. To overcome these limitations, we present a physiological functional method that provides objective and quantitative measurements of disease progression, enabling both early detection and precise measurements for research applications. This method allowed us to (1) quantify the virulence and pathogenicity levels of two Fol strains, as well as (2) to compare the susceptibility levels of different tomato cultivars. Notably, we were also able to (3) detect Fol infection at an early stage, before the appearance of visual symptoms.

Quantification of disease severity: Host susceptibility and pathogen virulence

Our study provides a new approach for quantifying pathogen aggressiveness in plants by using transpiration decrease as a comparative test for *Fol* virulence. We found that vF caused a significantly greater decrease in transpiration than mvF (Fig. 1c), indicating a higher level of pathogen aggressiveness. This was confirmed by traditional methods such as visual assessment of plants when symptoms appeared (Fig. 1d) and visual ratings of the level of infection in seedlings (Fig. S3). However, visual ratings of *Fol* were challenging due to the difficulty in comparing, assessing and scoring the disease severity. Stewart and McDonald (2014) demonstrated the divergences between scorers' visual assessments and the accurate values (Stewart & McDonald, 2014). Other researchers have also recognized the need for quantitative measures of pathogen aggressiveness, as visual estimation alone is insufficient (Bock et al., 2020; Gale et al., 2003; Ilgen et al., 2009). To the best of our knowledge, this is the first study to use whole-plant transpiration and continuous biomass assessments to assess pathogen virulence. Our results suggest that this approach could be a valuable tool for comparative testing of *Fol* strains.

The literature defines the M82 tomato as moderately resistant (Sela-Buurlage et al., 2001) or tolerant of *Fol*, race 2; whereas R13 is known to be susceptible to *Fol*, race 2 (Sarfatti et al., 1989). Despite these dichotomic definitions used to categorize a plant as either tolerant or susceptible to a pathogen, there remains a need for more quantitative, reliable and effective measurement techniques to improve our understanding of tolerance levels (as reviewed by Robb, 2007). Additionally, for vascular wilt disorders, disease severity is usually scored in a semi-

quantitative fashion using a disease index (Robb, 2007), as presented in Figure 1e. Although measuring disease severity can be challenging, yield is considered less controversial and is a reliable test for plant health (Scott, 2005). Our functional phenotyping method allows the classification of resistance-susceptibility on a percentage scale, as opposed to a dichotomous terminology. For instance, infected M82 plants exhibited a 15% decrease in plant weight; whereas infected R13 plants exhibited a weight decrease of 67% (Fig. 3b). Thus, the quantitative, objective nature of our functional phenotyping method significantly refines the evaluation of plant tolerance level, which could provide valuable insights into cultivar–pathogen dynamics and the risks and opportunities associated with those dynamics.

We posit that our findings likely correlate with plant performance in agricultural settings. Transpiration is intrinsically linked with CO_2 absorption, photosynthesis, plant growth and yield. The correlation between transpiration and crop yield is complex, as both factors are influenced by a multitude of environmental and physiological processes. Nevertheless, in many modern crops, whole-plant transpiration has been found to be linearly correlated with yield (Gosa et al., 2019). This relationship is particularly evident in tomato (Chaka Gosa et al., 2022), indicating that our functional phenotyping method may serve as a reliable prediction for productivity in that crop.

The cost of resistance

Constitutive activation of defense mechanisms might negatively affect plant productivity in the absence of pathogen infection (Zhao et al., 2017). In all of our experiments, the susceptibility or tolerance level of the plant was calculated as the difference between each infected line of plants and its non-inoculated control. Interestingly, these controls revealed a resistance cost: Non-inoculated M82 was less productive than non-inoculated R13 (19% less biomass, Fig. 3b) and non-inoculated MT was less productive than non-inoculated Mv (24% less transpiration, Fig. 3c) and MM (n.s., 17% less biomass, Fig. S4). At this point, since MM and MT (the isogenic lines) were not significantly different from one another, we cannot fully conclude that the lower yields of the pathogen-free tomato plants are the result of a tolerance cost. A similar resistance penalty was reported by Shteinberg et al. (2021), who found that tomato lines that were susceptible to *Tomato yellow leaf curl virus* performed better under optimal conditions than a resistant line (Shteinberg et al., 2021).

This penalty might be related to plant defense mechanisms. These mechanisms are considered costly as they divert energy and resources away from other plant processes (e.g., growth and reproduction). Thus, in the absence of pathogens, plants that activate fewer or less intense defense mechanisms are likely to be more productive than their well-defended counterparts (Cipollini et al., 2014; Herms & Mattson, 2015). This implies that the tolerant or resistant plants pay some potential yield penalty under optimal growth conditions. Our approach allows us to quantify and highlight these costs of resistance, as well as to quantify their spectrum, which could be considered from an economical perspective. We suggest that this quantification may be useful for breeders and farmers, helping them to fine-tune their selections and to invert their dichotomic scope of resistance-susceptible terminology to levels of productivity, risk and cost.

Early detection of disease

Our findings suggest that transpiration serves as an early indicator of *Fol* and *P. infestans* infection. Notably, in the case of *Fol*, this indication came up to 49 days before the manifestation of visual symptoms (Table 1, Row 7) and an average of 35.2 days before any morphological symptoms were observable. Other studies have reported a decline in vascular flow or water loss slightly before the appearance of wilt symptoms in infected plants (Feng et al., 2022; Street & Cooper, 1984; Wang et al., 2012). To document this, Wang et al. (2012) and Feng et al. (2022) used a Li-6400 gas exchange system (Li-Cor Inc.); whereas Street and Cooper (1984) used a Scholander pressure bomb. In contrast to the simple assessment using the PlantArray system, the aforementioned methods are time-consuming and laborious.

The decrease in the transpiration of the infected plants could be due to hydraulic blockage resulting from physical clogging of the xylem by insoluble fungal materials, such as spores, mycelia and polysaccharides. It also could be due to a signaling response pathway activated by a soluble fungal toxin that may have traveled through the vascular system to the leaves. Our observation that transpiration, K_{leaf} and water potential were all reduced following the exposure of leaves to fungal filtrate (Fig. 4) highlights the considerable impact of the signaling pathway on the plant's overall water balance. Researchers have tested the effects of the crude fungal toxins on wilting (Madhosingh, 1995), the death of leaf protoplasts (Sutherlandt & Pegg, 1992) and callus growth in culture media (Scala et al., 1985). However, to the best of our knowledge, this is the first study to examine the effect of fungal toxins on actual leaf hydraulic conductance. Our

findings suggest that the signaling pathway plays a crucial role in the plant's early response, affecting it even before any physical clogging occurs.

Interestingly, the vF toxins secreted into the media had a more severe effect than the mvF toxins, and leaves with high levels of immunity were less affected than susceptible leaves. This aligns with previous research involving culture filtrates, in which plant lines capable of tolerating or resisting toxins as seedlings or protoplasts also exhibited resistance under greenhouse conditions (Hartman et al., 1984; Mcleod & Smith, 2012; Sutherlandt & Pegg, 1992). Therefore, the impact of these toxins on plant hydraulics is similar to the effect of fungal infection. As documented previously, *Fol* increases xylem hydraulic resistance (Duniway, 1971)**.** The plant cellular regulation mechanism for fungal detection has been suggested to involve specific receptors, AtCERK1, AtLYK4 and notably AtLYK5, which have been shown to play key roles in the plant's response to chitin. This mechanism has been shown to be important in regulating K_{leaf}, particularly within the vascular bundle sheath and mesophyll cells (Attia et al., 2019).

Impact of environmental factors and plant–fungus interactions on disease progression

Our research underscores the significant effects of environmental factors and plant–fungus interaction in disease progression in the *Fol*–tomato pathosystem. Through the analysis of multiple experiments (Table S1) involving plant properties and environmental conditions, we gained valuable insights into the generation of optimal disease conditions (Model S1). Our findings suggest that smaller plants have a greater likelihood of exhibiting wilting symptoms within 30–70 days after inoculation. Similarly, early infected plants with *Tomato spotted wilt virus* (TSWV) displayed a greater percentage of leaves with symptoms than later infected ones (Rowland et al., 2005). Environmental factors such as high DLI and high RH were also observed to promote disease development, as expected. These findings emphasize the significance of considering early post-infection environmental factors and the interaction between plant type and fungal strain, as well as the initial plant weight when predicting the development of wilt symptoms. However, it is crucial to note that, despite the overall significance of our symptom-occurrence prediction model (Model S1; $R^2 = 1$, Pv < 0.001), the observed coefficients (directionality of the parameters) were not statistically significant (ChiSq = 0, Pv = 0.99). This lack of significance is likely due to the small number of repetitions within each plant–pathogen group. Therefore, these findings should be approached with caution and future studies with larger sample sizes are necessary to validate and further explore these potential associations.

Conclusions

Our study revealed that a high-throughput physiological monitoring system is suitable for the early detection and quantification of *Fusarium* wilt disease in tomato caused by *Fol*. Fundamentally, we found that whole-plant transpiration is a reliable indicator of plant health. Furthermore, the examined system also allows for simultaneous real-time analysis, which enables a quality comparison between pathogen virulence and host susceptibility. Indeed, the high-throughput monitoring of the physiological responses of tomato plants following infection with *Fol* revealed a spectrum of plant–pathogen interactions. This system may help breeders and researchers to evaluate plant tolerance and pathogen virulence on a quantitative scale, thereby making plant–pathogen research more efficient and more accurate. Further studies should be done to assess whether this system may be applied to other pathosystems. In addition, this approach generates large, annotated datasets of plant–pathogen–environment interactions, which could potentially be integrated into computer-based models for predicting plant reactions and estimating plant losses using machine learning and artificial-intelligence tools. Overall, this non-destructive, high-throughput method for monitoring plant health and disease progression has great potential for improving research in the field of phytopathology. Additionally, our study demonstrates the applicability of this physiological monitoring system for early detection and quantification of *P. infestans* infection in potato, offering a versatile tool for plant-health assessment in diverse pathosystems.

Acknowledgments

This research was supported by the Shoenberg Research Center for Agricultural Science (Grant #3175006230) and the Israel Science Foundation (Grant No. 1043/20). We extend our gratitude to Yael Rekah from the Hebrew University, Israel, for kindly providing seeds originally sourced from H. Laterrot, INRA, France. Special thanks to Dr. Yaniv Rotem (Hazera Genetics) for supplying *Fol* strain fr2T and offering valuable advice. We also acknowledge Nofit Vaknin, Phytopathology Coordinator (Hazera seeds), for her insights into traditional screening methods.

Competing interests

None declared.

Author Contributions

S.F. played a pivotal role in the planning and formulation of hypotheses, conducted all of the experiments, prepared graphs, performed statistical analysis, managed plant growth and post-harvest analyses and was a primary contributor to the writing of this manuscript. A.D. was responsible for measuring leaf hydraulic conductance and analyzing filtrate toxins and contributed to the manuscript review. D.B. played a major role in designing and performing the experiments, particularly with regard to the PlantArray system. S.B. contributed to the development of the hypotheses and provided critical input and suggestions in reviewing the manuscript. Y.S. was actively involved in conducting the experiments and data analysis. M.H. and S.R. collaboratively designed and executed the *Phytophthora infestans* experiments, oversaw pathogen growth and co-wrote relevant sections of the manuscript. E.M.H. managed all laboratory preparations, ensuring the efficient progress of the experimental work. S.C. contributed his extensive experience with *Fol* to various aspects of this research, including hypothesis development, experimental design and manuscript writing and review. M.M., as the principal investigator, managed the project, contributed to hypothesis generation, experimental design, data analysis and writing and reviewing the manuscript.

Data availability

The data that support the findings of this study are available from the corresponding author upon reasonable request. Additionally, some of the data can be found in the supplementary material for this article.

References

Attia, Z., Dalal, A., & Moshelion, M. (2020). Vascular bundle sheath and mesophyll cells modulate leaf water balance in response to chitin. *Plant Journal*, *101*(6), 1368–1377. https://doi.org/10.1111/TPJ.14598

Bock, C. H., Barbedo, J. G. A., Del Ponte, E. M., Bohnenkamp, D., & Mahlein, A.-K. (2020). From visual estimates to fully automated sensor-based measurements of plant disease severity: status and challenges for improving accuracy. *Phytopathology Research*, *2*(1), 1–30. https://doi.org/10.1186/S42483-020-00049-8

CABI - Global Burden of Crop Loss. (n.d.). Retrieved January 4, 2021, from https://www.cabi.org/projects/global-burden-of-crop-loss/

643 Chaka Gosa, S., Koch, A., Shenhar, I., Hirschberg, J., Zamir, D., & Moshelion, M. (2022). The
644 potential of dynamic physiological traits in young tomato plants to predict field-yield
645 performance. *Plant Science*, *315*(111122). https://doi.org/10.1016/j.plantsci.2021.111122

646 Cipollini, D., Walters, D., & Voelckel, C. (2014). Cost of resistance in plants: From theory to
647 evidence. *Annual Plant Reviews*, *47*, 263–307.
648 https://doi.org/10.1002/9781119312994.apr0512

649 Cohen, R., Milo, S., Sharma, S., Savidor, A., & Covo, S. (2019). Ribonucleotide reductase from
650 Fusarium oxysporum does not Respond to DNA replication stress. *DNA Repair*,
651 *83*(102674). https://doi.org/10.1016/j.dnarep.2019.102674

652 Cohen, Y. (2020). Root treatment with oxathiapiprolin, benthiavalicarb or their mixture provides
653 prolonged systemic protection against oomycete foliar pathogens. *PLOS One* .
654 https://doi.org/10.1371/journal.pone.0227556

655 Dalal, A., Shenhar, I., Bourstein, R., Mayo, A., Grunwald, Y., Averbuch, N., Attia, Z., Wallach,
656 R., & Moshelion, M. (2020). A telemetric, gravimetric platform for real-time physiological
657 phenotyping of plant–environment interactions. *Journal of Visualized Experiments*,
658 *162*(e61280), 1–28. https://doi.org/10.3791/61280

659 Dong, X., Ling, N., Wang, M., Shen, Q., & Guo, S. (2012). Fusaric acid is a crucial factor in the
660 disturbance of leaf water imbalance in Fusarium-infected banana plants. *Plant Physiology*
661 *and Biochemistry*, *60*, 171–179. https://doi.org/10.1016/j.plaphy.2012.08.004

662 Duniway, J. M. (1971). Resistance to Water Movement in Tomato Plants infected with
663 Fusarium. *Nature*, *230*, 252–253. https://doi.org/10.1038/230252a0

664 Eshed, Y., & Zamir, D. (1995). An introgression line population of Lycopersicon pennellii in the
665 cultivated tomato enables the identification and fine mapping of yield- associated QTL.
666 *Genetics*, *141*(3), 1147–1162. https://doi.org/10.1093/genetics/141.3.1147

667 Fang, Y., & Ramasamy, R. P. (2015). Current and prospective methods for plant disease
668 detection. In *Biosensors* (Vol. 5, Issue 3, pp. 537–561). MDPI AG.
669 https://doi.org/10.3390/bios5030537

670 Feng, H., Gonzalez Viejo, C., Vaghefi, N., Taylor, P. W. J., Tongson, E., & Fuentes, S. (2022).
671 Early Detection of Fusarium oxysporum Infection in Processing Tomatoes (Solanum
672 lycopersicum) and Pathogen–Soil Interactions Using a Low-Cost Portable Electronic Nose
673 and Machine Learning Modeling. *Sensors*, *22*(22), 8645.
674 https://doi.org/10.3390/S22228645/S1

675 Gale, L. R., Katan, T., & Kistler, H. C. (2003). The Probable Center of Origin of Fusarium
676 oxysporum f. sp. lycopersici VCG 0033. *Plant Disease*, *87*(12), 1433–1438.
677 https://doi.org/10.1094/PDIS.2003.87.12.1433

678 Gaunt, R. E. (1995). The relationship between plant disease severity and yield. *Annual Review of*
679 *Phytopathology*, *33*, 119–144. https://doi.org/10.1146/ANNUREV.PY.33.090195.001003

Gosa, S. C., Lupo, Y., & Moshelion, M. (2019). Quantitative and comparative analysis of whole-plant performance for functional physiological traits phenotyping: New tools to support pre-breeding and plant stress physiology studies. *Plant Science*, *282*, 49–59. https://doi.org/10.1016/J.PLANTSCI.2018.05.008

Grunwald, Y., Wigoda, N., Sade, N., Yaaran, A., Torne, T., Gosa, S. C., Moran, N., & Moshelion, M. (2021). Arabidopsis leaf hydraulic conductance is regulated by xylem sap pH, controlled, in turn, by a P-type H+-ATPase of vascular bundle sheath cells. *Plant Journal*, *106*(2), 301–313. https://doi.org/10.1111/TPJ.15235

Halperin, O., Gebremedhin, A., Wallach, R., & Moshelion, M. (2017). High-throughput physiological phenotyping and screening system for the characterization of plant–environment interactions. *Plant Journal*, *89*(4), 839–850. https://doi.org/10.1111/tpj.13425

Hartman, C. L., Mccoy, T. J., & Knous, T. R. (1984). Selection of alfalfa (Medicago sativa) cell lines and regeneration of plants resistant to the toxin(s) produced by Fusarium oxysporum f. sp. hiedicaginis*. *Plant Science Letters*, *34*, 183–194. https://doi.org/10.1016/0304-4211(84)90141-X

Herms, D. A., & Mattson, W. J. (2015). The Dilemma of Plants: To Grow or Defend. *Https://Doi.Org/10.1086/417659*, *67*(3), 283–335. https://doi.org/10.1086/417659

Hipsch, M., Lampl, N., Zelinger, E., Barda, O., Waiger, D., & Rosenwasser, S. (2021). Sensing stress responses in potato with whole-plant redox imaging. *Plant Physiology*, *187*(2), 618–631. https://doi.org/10.1093/PLPHYS/KIAB159

Hipsch, M., Michael, Y., Lampl, N., Sapir, O., Cohen, Y., Helman, D., & Rosenwasser, S. (2023). Early detection of late blight in potato by whole-plant redox imaging. *Plant Journal*, *113*(4), 649–664. https://doi.org/10.1111/TPJ.16071

Ilgen, P., Hadeler, B., Maier, F. J., & Schäfer, W. (2009). Developing kernel and rachis node induce the trichothecene pathway of fusarium graminearum during wheat head infection. *Molecular Plant-Microbe Interactions*, *22*(8), 899–908. https://doi.org/10.1094/MPMI-22-8-0899

Kashyap, A., Planas-Marquès, M., Capellades, M., Valls, M., & Coll, N. S. (2021). Blocking intruders: inducible physico-chemical barriers against plant vascular wilt pathogens. *Journal of Experimental Botany*, *72*(2), 184–198. https://doi.org/10.1093/jxb/eraa444

Madden, L. V., Hughes, G., & Bosch, F. (2007). *The Study of Plant Disease Epidemics*. The American Phytopathological Society.

Madhosingh, C. (1995). Relative wilt-inducing capacity of the culture filtrates of isolates of Fusarium oxysporum f.sp. radids-lycopersici, the tomato crown and root rot pathogen. *J. Phytopathology*, *143*, 193–198.

Martinelli, F., Scalenghe, R., Davino, S., Panno, S., Scuderi, G., Ruisi, P., Villa, P., Stroppiana, D., Boschetti, M., Goulart, L. R., Davis, C. E., & Dandekar, A. M. (2015). Advanced

methods of plant disease detection. A review. *Agronomy for Sustainable Development*, *35*(1), 1–25. https://doi.org/10.1007/s13593-014-0246-1

Mcleod, A. G., & Smith, H. C. (2012). Verticillium wilt of tobacco. The effect of culture filtrates of Verticillium dahliae Kleb. on tobacco. *New Zealand Journal of Agricultural Research*, *4*(2), 123–128. https://doi.org/10.1080/00288233.1961.10419925

Muraguchi, H., Ito, Y., Kamada, T., & Yanagi, S. O. (2003). A linkage map of the basidiomycete Coprinus cinereus based on random amplified polymorphic DNAs and restriction fragment length polymorphisms. *Fungal Genetics and Biology*, *40*(2), 93–102. https://doi.org/10.1016/S1087-1845(03)00087-2

Nemec, S., Syversten, J., & Levy, Y. (1986). Water relations of rough lemon (Citrus jambhiri Lush.) citrus seedlings infected with Fusarium solani. *Plant and Soil*, *93(2)*, 231–239. https://doi.org/https://doi.org/10.1007/BF02374225

Portal, N., Soler, A., Alphonsine, P. A. M., Borras-Hidalgo, O., Portieles, R., Peña-Rodriguez, L. M., Yanes, E., Herrera, L., Solano, J., Ribadeneira, C., Walton, J. D., & Santos, R. (2018). Nonspecific toxins as components of a host-specific culture filtrate from Fusarium oxysporum f. sp. cubense race 1. *Plant Pathology*, *67*(2), 467–476. https://doi.org/10.1111/PPA.12736

Prashant, M. k., Roland, F. T. V., & Alastair, C. (2003). Development of a PCR-based assay for rapid and reliable identification of pathogenic Fusaria. *FEMS Microbiology Letters*, *218*(2), 329–332. https://doi.org/10.1111/J.1574-6968.2003.TB11537.X

Rep, M., Meijer, M., Houterman, P. M., Van Der Does, H. C., & Cornelissen, B. J. C. (2005). Fusarium oxysporum evades I-3-mediated resistance without altering the matching avirulence gene. *MPMI*, *18*(1), 15–23. https://doi.org/10.1094/MPMI-18-0015

Robb, J. (2007). Verticillium tolerance: resistance, susceptibility, or mutualism? *Canadian Journal of Botany*, *85*(10), 903–910. https://doi.org/10.1139/B07-093

Sarfatti, M., Fluhr, R., & Zamir, D. (1989). An RFLP marker in tomato linked to the Fusarium oxysporum resistance gone 12. *Theor Appl Genet*, *78*, 755–759. doi: 10.1007/BF00262574

Sarkozi, A. (2019, April 3). *FAO - News Article: New standards to curb the global spread of plant pests and diseases*. http://www.fao.org/news/story/en/item/1187738/icode/

Scala, A., Bettini, P., Buiatti, M., Bogani, P., Pellegrini, G., & Tognoni, F. (1985). Tomato-fusarium oxysporum f. sp. lycopersici interaction: "in vitro" analysis of several possible pathogenic factors. *Phytopath.*, *113*, 90–94. https://doi.org/10.1111/j.1439-0434.1985.tb00830.x

Sela-Buurlage, M. B., Budai-Hadrian, O., Pan, Q., Carmel-Goren, L., Vunsch, R., Zamir, D., & Fluhr, R. (2001). Genome-wide dissection of Fusarium resistance in tomato reveals multiple complex loci. *Molecular Genetic and Genomics*, *265*, 1104–1111. https://doi.org/10.1007/s004380100509

754 Shteinberg, M., Mishra, R., Anfoka, G., Altaleb, M., Brotman, Y., Moshelion, M., Gorovits, R.,
755 & Czosnek, H. (2021). Tomato yellow leaf curl virus (TYLCV) promotes plant tolerance to
756 drought. *Cells Communication*. https://doi.org/10.3390/cells10112875

757 Singh, V. K., Singh, H. B., & Upadhyay, R. S. (2017). Role of fusaric acid in the development of
758 'Fusarium wilt' symptoms in tomato: Physiological, biochemical and proteomic
759 perspectives. *Plant Physiology and Biochemistry*, *118*, 320–332.
760 https://doi.org/10.1016/j.plaphy.2017.06.028

761 Stewart, E. L., & McDonald, B. A. (2014). Measuring quantitative virulence in the wheat
762 pathogen Zymoseptoria tritici using high-throughput automated image analysis. *American*
763 *Phytopathological Society (APS)*, *104*(9), 985. https://doi.org/10.1094/PHYTO-11-13-0328-
764 R

765 Street, P. F. S., & Cooper, R. M. (1984). Quantitative measurement of vascular flow in petioles
766 of healthy and Verticillium-infected tomato. *Plant Pathology*, *33*(4), 483–492.
767 https://doi.org/10.1111/J.1365-3059.1984.TB02872.X

768 Sutherlandt, M. L., & Pegg, G. F. (1992). The basis of host recognition in Fusarium oxysporum
769 f. sp. lycopersici. *Physiological and Molecular Plant Pathology*, *40*, 423–436.
770 https://doi.org/10.1016/0885-5765(92)90033-R

771 Taylor, A., Vágány, V., Jackson, A. C., Harrison, R. J., Rainoni, A., & Clarkson, J. P. (2016).
772 Identification of pathogenicity-related genes in Fusarium oxysporum f. sp. cepae. *Molecular*
773 *Plant Pathology*, *17*(7), 1032–1047. https://doi.org/10.1111/MPP.12346

774 van der Does, H. C., Constantin, M. E., Houterman, P. M., Takken, F. L. W., Cornelissen, B. J.
775 C., Haring, M. A., van den Burg, H. A., & Rep, M. (2019). Fusarium oxysporum colonizes
776 the stem of resistant tomato plants, the extent varying with the R-gene present. *European*
777 *Journal of Plant Pathology*, *154*(1), 55–65. https://doi.org/10.1007/s10658-018-1596-3

778 Wang, M., Ling, N., Dong, X., Zhu, Y., Shen, Q., & Guo, S. (2012). Thermographic
779 visualization of leaf response in cucumber plants infected with the soil-borne pathogen
780 Fusarium oxysporum f. sp. cucumerinum. *Plant Physiology and Biochemistry*, *61*, 153–161.
781 https://doi.org/10.1016/J.PLAPHY.2012.09.015

782 Wang, M., Sun, Y., Sun, G., Liu, X., Zhai, L., Shen, Q., & Guo, S. (2015). Water balance altered
783 in cucumber plants infected with Fusarium oxysporum f. sp. cucumerinum. *Scientific*
784 *Reports*, *5*. https://doi.org/10.1038/srep07722

785 Zhao, M., Ji, H.-M., Gao, Y., Cao, X.-X., Mao, H.-Y., Liu, P., & Ouyang, S.-Q. (2017).
786 Comparative transcriptome profiling conferring of resistance to Fusarium 1 oxysporum
787 infection between resistant and susceptible tomato. *BioRxiv*. https://doi.org/10.1101/116988

788 Zolan, M. E., & Pukkila, P. J. (1986). Inheritance of DNA Methylation in Coprinus cinereus.
789 *Molecular and Cellular Biology*, *6*(1), 195–200. https://doi.org/10.1128/MCB.6.1.195-
790 200.1986

Supporting Information

Fig. S1 Weather properties continually monitored in the greenhouse.

Fig. S2 A classic seedling disease assay confirmed the resistance of MT and the susceptibility of MM, R13 and M82 to *Fol*.

Fig. S3 A classic seedling disease assay confirmed that vF is more virulent than mvF.

Fig. S4 Plants of susceptible (MM, gray) and resistant (MT, black) near-isogenic lines were inoculated with vF (dashed line).

Fig. S5 Effects of chitin and ABA on the hydraulics of leaves detached from MM and MT plants.

Fig. S6 Effects of toxins released from the moderately virulent and virulent *Fol* strains on leaves detached from MM and MT tomato plants.

Table S1 Summary of experiments with different *Fol* strains and plants of varying levels of susceptibility.

Model S1 Logistic regression model of symptom occurrence.